Data Predistortion for Multicarrier Satellite Channels Based on Direct Learning

Roberto Piazza, *Student Member, IEEE,* Bhavani Shankar, M. R, *Member, IEEE,* and Bjorn Ottersten, *Fellow, IEEE*

***Abstract*—Satellite communication is facing the urgent need of improving data rate and efficiency to compete with the quality of service offered by terrestrial communication systems. An imminent gain, achievable without the need of upgrading current satellite technology, can be obtained by exploiting multicarrier operation at the transponder and using highly efficient modulation schemes. However, on-board multicarrier joint amplification of high order modulation schemes is a critical operation as it brings severe non-linear distortion effects. These distortions increase as the on-board High Power Amplifier (HPA) is operated to yield higher power efficiencies. In this work, we propose novel techniques to implement on ground predistortion that enable multicarrier transmission of highly efficient modulation schemes over satellite channels without impacting infrastructure on the downlink.**

***Index Terms*—Non-linear distortions, intermodulation products, multicarrier predistortion, memory polynomials, direct estimation, adaptive algorithm, satellite communication.**

I. Introduction

THERE is a strong interest in increasing the data rate over satellite channels while reducing the cost through optimizing payload architecture and mass requirements. This has motivated the quest for spectrally efficient transmissions while sharing a single high power amplifier (HPA) among multiple carriers. On-board power amplification, a key satellite operation, is inherently non-linear and leads to severe distortions when combined with higher modulation. These effects take the form of inter-symbol interference (ISI) and adjacent channel interference (ACI). Joint amplification of multiple carriers produces intermodulation products (IMD) that excite strong ACI, while the non-linear characteristic of the amplifier combined with the memory effects of the channelization filters generates ISI [1]. Reducing the on-board amplifier power efficiency not only increases the equivalent cost per bit, but also limits the transmission rate due to a reduction in the received signal to noise ratio. Moreover, when multilevel modulation schemes are used in such a multicarrier scenario, the generated distortion can be so significant that the joint amplification cannot be pursued. Hence multicarrier signals have to be limited to single ring modulation schemes, such as QPSK and 8PSK, thereby penalizing spectral efficiency further.

In order to maximize the transponder throughput along with the HPA power efficiency, additional processing techniques have to be put in place. On-board processing is usually not an economically as well as technologically convenient solution as it is not amenable for upgrades during the satellite mission lifetime (usually 15 years). This motivates on-ground interference mitigation. Transmitter processing techniques, known as digital predistortion (DPD), pre-process the transmitted signal in order to reduce the interference at the receiver. On the other hand, receiver techniques, generally known as equalization, aim to recover the transmitted signal by mitigating interference. In most of the current satellite applications, such as TV broadcasting, the receivers are legal TV decoders and they cannot support joint processing of multiple carriers. This is due to the fact that only one carrier is usually decoded, and the complexity, as well as the cost, of receivers is also limited by the market needs. On the other hand, the multicarrier signal is uplinked at the Gateway (GW) that has access to all carriers. Further, a GW can sustain the added computational complexity while seamlessly integrating the multiple carrier operation. This consideration defines a satellite scenario where the multicarrier signal is predistorted at the gateway without any impact on the existing receiver architectures. Thus the chosen scenario precludes the use of multiple carrier receiver architectures proposed in [2], [3]. However, the seminal characterization of non-linear interference detailed in [2], [3] is fundamental to the current work.

The objective of the predistortion function is to reduce the level of interference, optimize the power efficiency of the on-board HPA and improve the spectral efficiency [4]. In general, the predistorter implements the channel inverse function. The traditional Look up table (LUT) based predistortion has been considered in [5], [6]. On the other hand, single carrier model based predistorters [4] have been studied extensively in literature. Exploiting the Volterra representation of non-linear channels with memory [7], the predistorter can itself be modelled using a Volterra series [8]. While Volterra series provides for a complete representation, the large number of parameters [8] makes it less attractive in common applications. Memory polynomials (MP) is a simplification of the full Volterra series that completely models a parallel Hammerstein system [9], [10]. In terrestrial applications, memory polynomials have become popular as effective predistortion techniques for single carrier channels, since they significantly reduce the complexity compared to the full Volterra representation suffering only a minor degradation in performance [11], [12]. Recently published single carrier predistortion techniques based on linear piecewise basis functions [13] provide lower sensitivity to estimation noise. Single carrier predistortion has been applied

R. Piazza, B. Shankar and B. Ottersten are with the Interdisciplinary Centre for Security, Reliability and Trust, (SnT), University of Luxembourg (see http://wwwfr.uni.lu/snt). This work is supported by AFR PhD grant N4878123 from the *Fonds National de la Recherche Luxembourg.*

either at the signal level [9]–[11] or at the data/symbol level [5], [14]. Signal predistortion is suitable in applications where the amplifier and the predistorter are co-located and aims to reduce both the received interference and the spectral leakage of the amplified signal [11]. However, signal predistorter per-se is wideband non-linear processing and causes bandwidth expansion on of the predistorted signal [11]. In satellite channels, the HPA is on-board, and the tight out-of-band emission constraints applied on the uplinked signal preclude the application of on-ground signal predistortion as such. On the other hand, data predistortion can reduce interferences to some certain extent and it does not introduce spectral regrowth on the predistorted signal [5]. Thus the use of data predistortion has the advantage of not-violating the uplink regulations. Notice that the downlink out-of-band emission constraints are satisfied by the OMUX filter that, according to regulations, eliminates the spectral regrowth generated by the on-board HPA.

While single carrier predistortion is well explored in the literature, multicarrier predistortion has received less attention: A dual carrier signal predistortion based on a simplified version of memory polynomials is provided in [15] for terrestrial applications. Multicarrier predistortion for satellite channels has been firstly addressed in [16] where joint data predistortion based on memory polynomials is considered. Using a similar approach, orthogonal bases functions for reduced complexity multicarrier predistorion have been proposed in [17].

Key to the performance of the given predistorter model is the ability to estimate the coefficients with high fidelity [18]. Two paradigms for the estimation of DPD coefficients are explored in literature. The well known *indirect estimation* of the parameters leads to a post-channel inverse function as predistorter [9], [11]. This approach has a limited complexity but does not guarantee optimal performance with respect to the selected model [18]. On the other hand, the *direct estimation* method [12] leads to a predistorter function that resembles the channel pre-inverse function and provides better performance compared to indirect methods. Further, the direct method is shown to be robust to estimation noise [18], thereby easing the design requirements. While indirect methods have been considered for both single carrier and multicarrier scenarios [11], [16], the direct method has been considered only for single carrier scenario [12] where the parameter estimation is performed through the well known Recursive Least Squares (RLS) and Least Mean Squares (LMS) algorithms.

In this work, we consider the *direct estimation* problem in the context of multicarrier satellite channels and present two novel optimization methods, namely *Individual* and *Joint* predistorter design, for estimation of predistorter parameters. The first method extends [12] by designing predistorters for each of the carriers individually, while a joint optimization of the predistorter parameters across carriers is undertaken in the latter method. Due to their formulation, these methods provide a complexity performance trade-off offering certain flexibility to the system designer. Building on the multicarrier Volterra model derived in [3] and the direct method estimation for single carrier provided in [12], we design novel adaptive multicarrier data predistortion mechanisms based on the low complexity memory polynomial model. Iterative algorithms are considered: RLS and LMS formulations for the parameter estimation have been derived and their convergence studied. Numerical evaluation of the techniques indicate a superior performance and robustness to noise of the proposed direct estimation compared to existing algorithms.

Notation: $\boldsymbol{a}$ and $\mathbf{A}$ respectively denote vectors and matrices, ^{T},* denote the transposition and complex conjugation operations, $\otimes$ Kronecker product and $E(\cdot)$ refers to ensemble averaging. Further $\|\cdot\|$ refers to the l_2 norm.

II. Multicarrier Satellite Channel with single on-board HPA

A. Scenario

A Ku-band broadcasting application to fixed users employing a single geostationary (GEO) satellite is considered. Further, a single GW is assumed to uplink multiple carriers to the GEO satellite where the composite signal will be processed by a single transponder. Each carrier provides an independent service; in a typical application different carriers could be relevant to different geographical location. Further, in common commercial applications such as TV broadcast, each User Terminal (UT) can only decode its intended carrier.

B. System Model

In Fig. 1 we illustrate the overall multicarrier system model comprising a transmitting gateway, the satellite transponder and the on-ground receivers. The gateway performs the predistortion function and subsequently uplinks all the carriers. Let $u_m(n)$ be the modulated symbol on carrier m at the nth instance. The predistorted symbol of the mth carrier at the nth instance, denoted by $x_m(n)$, is obtained by jointly processing $\{u_m(n-k)\}_{m=1}^{M}$ with $-K < k < K$ where K indicates the (two sided) memory depth and M is number of carriers. Notice that if predistortion is not applied (no compensation) we simply have the identity $x_m(n) = u_m(n)\ \forall m, n$. The satellite transponder for multicarrier application includes wideband input and output multiplexing filters, namely IMUX and OMUX, and the HPA. The IMUX is used to eliminate out-of-band noise injection while OMUX is used to reduce out-of-band emission. The filter responses are extracted from [5], while we consider the well known Saleh model for the HPA [19]. The Saleh model is characterized by the AM/AM and AM/PM curves given by $A(r) = \frac{2r}{1+r^2}; \Phi(r) = \frac{\pi}{6}\frac{r^2}{1+r^2}$, respectively. Focusing on the non-linear impairments excited by the multicarrier application, we consider AWGN for the downlink. Since UT that can only decode its intended carrier, joint processing or multiple carriers cannot be supported by the receivers. Therefore, in order to target a realistic and commercially convenient scenario, in this study we do not consider any multi carrier equalization technique.

C. Non-linear Channel Distortion Analysis

The aforementioned satellite channel can be modelled as a *non-linear system with memory* leading to constellation warping, ISI and ACI. The effect of these impairments are

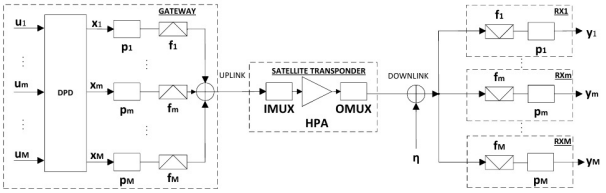

Fig. 1. System model for a non-linear satellite channel with M carriers

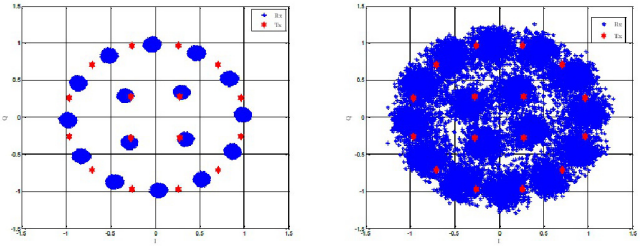

Fig. 2. Scatter plots corresponding to single carrier (left) and multicarrier (right) signals for a five carrier noiseless non-linear satellite channel with Output Back Off (OBO)=3.6 dB

depicted in Figure 2 where the noiseless scatter plot of the 16 APSK modulated symbols received on the central carrier of a three carrier system is illustrated for the case of no compensation. The corresponding effect for the single carrier channel is also shown to highlight the significant increase of interference due to ACI and further motivate the need of specific countermeasures. Recalling that $u_m(n)$ is the modulated symbol on carrier m at time n, we define,

$$\boldsymbol{u}(n) = [u_1(n), \ldots, u_M(n)]^T, \quad (1)$$

$$\boldsymbol{u}_K(n) = [\boldsymbol{u}^T(n-K), \ldots \boldsymbol{u}^T(n+K)]^T, \quad (2)$$

where $\boldsymbol{u}(n)$ and $\boldsymbol{u}_K(n)$ are of dimensions $M \times 1$ and $(2K+1)M \times 1$ respectively. Here, $\boldsymbol{u}(n)$ is the vector of input symbols across M carriers at the instance n, while $\boldsymbol{u}_K(n)$ denotes a collection of $\boldsymbol{u}(n)$ for a specified time interval. We also define,

$$\boldsymbol{u}_K^{(d)}(n) = \underbrace{\boldsymbol{u}_K(n) \otimes \cdots \otimes \boldsymbol{u}_K(n)}_{\text{d times}}. \quad (3)$$

With these notations and considering a channel with no predistortion applied, we can express $y_m(n)$, the received symbols for the mth carrier at the nth sampling instance, using a general Volterra discrete time model [20] as

$$y_m(n) = y_m^{(1)}(n) + y_m^{(3)}(n) + y_m^{(5)}(n) + \ldots + \eta_m(n) \quad (4)$$

$$y_m^{(1)}(n) = \boldsymbol{g}_m^{(1)} \boldsymbol{u}_{K_1}{}^{(1)}(n) \quad (5)$$

$$y_m^{(3)}(n) = \boldsymbol{g}_m^{(3)} \mathbf{J}_m^{(3)} \boldsymbol{u}_{K_3}{}^{(2)}(n) \otimes [\boldsymbol{u}_{K_3}{}^{(1)}(n)]^* \quad (6)$$

$$y_m^{(5)}(n) = \boldsymbol{g}_m^{(5)} \mathbf{J}_m^{(5)} \boldsymbol{u}_{K_5}{}^{(3)}(n) \otimes [\boldsymbol{u}_{K_5}{}^{(2)}(n)]^*. \quad (7)$$

The row vectors $\boldsymbol{g}_m^{(p)}$ are the pth order Volterra kernel coefficients, $\eta_m(n)$ is the receiver noise on carrier m at nth instance and $\mathbf{J}_m^{(p)}$ is a selection matrix. In the complete Volterra representation, $\mathbf{J}_m^{(p)}$ corresponds to an identity matrix of dimension $((2K_p+1)M)^p$ where K_p is the (two sided) memory depth for degree p terms. However, such a representation has redundant terms like $u_1(n)u_2(n)u_3(n)^*$ and $u_2(n)u_1(n)u_3(n)^*$ and $\mathbf{J}_m^{(p)}$ can be used to eliminate redundant terms generated by the Kronecker products. In addition to providing a compact representation, $\mathbf{J}_m^{(p)}$ is used to select specific polynomial terms from the general model towards reducing the number of intermodulation products. In fact, the baseband model provided in (4) is valid only for intermodulation products that generate in-band distortion [3]. We define $\Omega_{m,d}$ as the set of intermodulation frequency products $(m_1, \ldots, m_d)$ of degree d that generate in band distortion to carrier m.

III. Memory Polynomial Predistortion and Channel Model

In this section, we define models used for the predistortion function and the non-linear channel. The channel model is described since it will be exploited in the estimation of the predistorter parameters.

A. Predistorter Model

We consider a memory polynomial model [16] for both the predistorter function and the channel model. This model is a special case of reduced complexity Volterra implementation where only the *diagonal* elements of the full model are considered. As documented in [3], the complexity of the Volterra model can be reduced by eliminating the kernel terms having negligible contribution (weight) while suffering only a minor loss in performance. In addition, to the best of authors' knowledge, a representation of the intermodulation products typical of the multicarrier non-linear channels [3] exists only for polynomial basis functions, thereby motivating their use.

The predistortion function is based on a complex polynomial function of the input symbols given by,

$$\phi_{m_1,\ldots,m_d}^{\{d\}}(\boldsymbol{u}(n)) = \prod_{j=1}^{(d+1)/2} u_{m_j}(n) \prod_{j=(d+1)/2+1}^{d} u_{m_j}^*(n), \quad (8)$$

where d is the polynomial degree and $(m_1, \ldots, m_d)$ are the selected product terms where each $m_i \in (1, \ldots, M)$. Recall that, for each carrier m and polynomial degree d, we have a specific set of in-band product terms enumerated in the set $\Omega_{m,d}$. This allows us to define,

$$\boldsymbol{\psi}_m^{\{d\}}(\boldsymbol{u}(n)) = \{\phi_{m_1,\ldots,m_d}^{\{d\}}(\boldsymbol{u}(n))\}_{(m_1,\ldots,m_d)\in\Omega_{m,d}}, \quad (9)$$

as the $|\Omega_{m,d}| \times 1$ vector comprising polynomial function evaluations corresponding to the carrier combinations causing in-band distortion. We further define,

$$\boldsymbol{\chi}_m^{\{d\}} = \Big[\Big[\boldsymbol{\psi}_m^{\{d\}}(\boldsymbol{u}(n-K_d))\Big]^T, \Big[\boldsymbol{\psi}_m^{\{d\}}(\boldsymbol{u}(n-K_d+1))\Big]^T, \ldots, \Big[\boldsymbol{\psi}_m^{\{d\}}(\boldsymbol{u}(n+K_d))\Big]^T\Big]^T, \quad (10)$$

where $\boldsymbol{\chi}_m^{\{d\}}$ is a $(2K_d+1)|\Omega_{m,d}| \times 1$ vector with (two sided) memory depth of K_d corresponding to degree d. Note that the

memory depth is implicitly used for ease of notation. Finally we stack all the terms corresponding to different degrees as,

$$\boldsymbol{\phi}_m(\boldsymbol{u}(n)) = \left[\left[\boldsymbol{\chi}_m^{\{1\}}\right]^T, \left[\boldsymbol{\chi}_m^{\{2\}}\right]^T, \ldots, \left[\boldsymbol{\chi}_m^{\{p\}}\right]^T\right]^T, \quad (11)$$

where $\boldsymbol{\phi}_m(\boldsymbol{u}(n))$ is now a $\sum_p (2K_p+1)|\Omega_{m,p}| \times 1$ dimensional vector.

Let $q_{m_1,\ldots,m_d}(k)$ denote the predistorter coefficient that will eventually weigh the basis function $\phi^{\{d\}}_{m_1,\ldots,m_d}(\cdot)$. Similar to (9), we first define,

$$\boldsymbol{q}_m^{\{d\}}(k) = \{q_{m_1,\ldots,m_d}(k)\}_{(m_1,\ldots,m_d)\in\Omega_{m,d}}, \quad (12)$$

to be a $|\Omega_{m,d}| \times 1$ coefficient vector corresponding to delay k. We further define,

$$\boldsymbol{z}_m^{\{d\}} = \left[\left[\boldsymbol{q}_m^{\{d\}}(-K_d)\right]^T, \ldots, \left[\boldsymbol{q}_m^{\{d\}}(K_d)\right]^T\right]^T, \quad (13)$$

where $\boldsymbol{z}_m^{\{d\}}$ is a $(2K_d+1)|\Omega_{m,d}| \times 1$ vector with K_d being the (two sided) memory depth of the predistorter function relative to degree d. We finally define the vector of predistorter coefficients for carrier m as,

$$\boldsymbol{w}_m = \left[\left[\boldsymbol{z}_m^{\{1\}}\right]^T, \ldots, \left[\boldsymbol{z}_m^{\{p\}}\right]^T\right]^T, \quad (14)$$

where $\boldsymbol{w}_m$ is a $\sum_p (2K_p+1)|\Omega_{m,p}| \times 1$ vector.

Having defined relevant quantities, the predistorter output $x_m(n)$ can now be defined similarly to [16] as an inner product between the non-linear input combination vector $\boldsymbol{\phi}_m$ and the kernel coefficients $\boldsymbol{w}_m$,

$$x_m(n) = \boldsymbol{w}_m^T \left[\boldsymbol{\phi}_m(\boldsymbol{u}(n))\right]. \quad (15)$$

A key aspect of the formulation is the linear dependence of $x_m(n)$ on $\boldsymbol{w}_m$, a fact that will be exploited later. The predistorted symbols $x_m(n)$ are then upsampled, filtered and transmitted through the non-linear channel (kindly refer to Fig. 1). Towards further analysis, a channel model relating $\{x_m(n)\}$ to the output is needed; this is taken up next.

B. Reduced Complexity Channel Model

Rather than the full Volterra representation of (4), we select the memory polynomial function to model the channel. Such a model has the same form as the predistorter. This choice is motivated by the nature of the satellite channel where the memory effects are minor [16]. Such a simplification lowers the number of parameters, thereby simplifying the analysis and reducing the complexity of implementation. Further, such a choice provides a formulation that could be easily generalized to the complete Volterra model. Similar to (15), we can then express the output of the channel as,

$$y_m(n) = \boldsymbol{h}_m^T \left[\boldsymbol{\phi}_m(\boldsymbol{x}(n))\right], \quad (16)$$

where $\boldsymbol{\phi}_m(\cdot)$ now takes predistorted symbols, $\boldsymbol{x}(n) = [x_1(n) \ldots x_M(n)]^T$, as inputs and $\boldsymbol{h}_m$ denotes the channel coefficients and are defined similarly to $\boldsymbol{w}_m$ in (14). With the channel model in place, we now briefly describe the estimation of the model parameters $\boldsymbol{h}_m$, which would be later used in the predistorter design.

1) Estimation of Channel Parameters: Given N samples of transmitted and received symbols, $\boldsymbol{x}(\cdot)$ and $y_m(\cdot)$ respectively, we consider minimizing, $\sum_{n=0}^{N-1} |y_m(n) - \boldsymbol{h}_m^T [\boldsymbol{\phi}_m(\boldsymbol{x}(n))]|^2$. Towards this, we stack these quantities to obtain,

$$\boldsymbol{v}_m = [y_m(0), \ldots, y_m(N-1)]^T, \quad (17)$$

$$\mathbf{Z}_m = \begin{bmatrix} [\boldsymbol{\phi}_m(\boldsymbol{x}(0))]^T \\ \vdots \\ [\boldsymbol{\phi}_m(\boldsymbol{x}(N-1))]^T \end{bmatrix}, \quad (18)$$

so that the minimization reduces to $\|\boldsymbol{v}_m - \mathbf{Z}_m \boldsymbol{h}_m\|^2$. The least squares solution for $\boldsymbol{h}_m$ is then straightforward, leading to,

$$\boldsymbol{h}_m = (\mathbf{Z}_m^H \mathbf{Z}_m)^{-1} \mathbf{Z}_m^H \boldsymbol{v}_m. \quad (19)$$

Instead of the block implementation provided in (19), an iterative approach based on the RLS is considered similarly to [12]. Such an implementation will iteratively improve the estimate of $\boldsymbol{h}_m$ and will be exploited in the sequel for the estimation of predistorter parameters. Having determined the necessary quantities, we now proceed with the central theme of estimating $\{\boldsymbol{w}_m\}_m$.

C. Estimation of Predistortion Parameters

Two methodologies to estimate the predistorter parameters are prevalent in the literature. These are the *indirect* and *direct* methods [11], [12]. Typically predistortion design assumes a system where the receiver is capable of feeding back training data to the transmitter [5]. In the current work, we assume the presence of a dedicated multicarrier receiver connected to the GW and relaying the requisite data for the estimation of predistortion parameters. These special receivers are operator installed and are different from the standard user terminals. Indirect estimation is illustrated in Fig. 3, where the post-

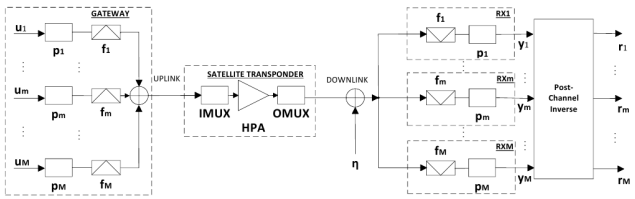

Fig. 3. Post-inverse Channel Estimation

inverse is modelled as $r_m(n) = \boldsymbol{w}_m^T [\boldsymbol{\phi}_m(\boldsymbol{y}(n))]$. Note here that the arguments of $\boldsymbol{\phi}_m(\cdot)$ are now the channel outputs, $\boldsymbol{y}(n) = [y_1(n), \ldots, y_M(n)]^T$. The methodology is to estimate $\boldsymbol{w}_m$ such that $E[|u_m(n) - r_m(n)|^2] \approx \frac{1}{N}\sum_{n=0}^{N-1} |u_m(n) - r_m(n)|^2$ is minimized for each $m \in (1, \ldots, M)$ and a given training sequence of length N. In other words, the channel inverse function with parameters $\boldsymbol{w}_m$ would process the channel output samples $\boldsymbol{y}(n)$ yielding, in the ideal case, the original input transmitted symbols $u_m(n)$. This is a standard Least Squares problem with a simple derivation and a low complexity implementation. Following the steps leading to the solution of $\boldsymbol{h}_m$ in (19), we can obtain

$$\boldsymbol{w}_m = (\boldsymbol{\Theta}_m^H \boldsymbol{\Theta}_m)^{-1} \boldsymbol{\Theta}_m^H \boldsymbol{s}_m \quad \text{Indirect Method} \quad (20)$$

where $\boldsymbol{s}_m = [u_m(0), \ldots, u_m(N-1)]^T$ and $\boldsymbol{\Theta}$ is similar to $\mathbf{Z}$ in (18) with $\boldsymbol{\phi}_m(\boldsymbol{x}(k))$ replaced by $\boldsymbol{\phi}_m(\boldsymbol{y}(k))$. Kindly note in the current work, the indirect learning architecture, as proposed originally in [8] is not implemented. Instead, similar to [11], we solve the post inverse LS estimation problem offline. It is important to point out that indirect estimation does not *directly* target the receiver error minimization defined as $E[|u_m(n) - y_m(n)|^2]$. However, it relies on the argument that the channel pre and post-inverses are equivalent. Such an argument has been proven in [7] for the single carrier case. The *direct* estimation method [12] overcomes this discrepancy and will be discussed in the following sections.

IV. Direct Estimation

A. Problem Formulation

We now discuss a different approach for the estimation of $\boldsymbol{w}_m$ that *directly* targets the minimization of the interference at the receiver $e_m(n) = u_m(n) - y_m(n)$. While the formulation of the direct estimation is straight forward in the single carrier, the case is not so for multicarrier scenario (refer to Fig. 4). We consider the following interesting formulations,

- M *Individual* cost functions:
  - $E[C(\boldsymbol{w}_m(n))]$ with $C(\boldsymbol{w}_m(n)) = |e_m(n)|^2, m \in (1, \ldots, M)$
- *Joint* cost function:
  - $E[C(\boldsymbol{w}_1(n), \ldots, \boldsymbol{w}_M(n))]$ with $C(\boldsymbol{w}_1(n), \ldots, \boldsymbol{w}_M(n)) = \sum_{m=1}^{M} |e_m(n)|^2$

Individual estimation of predistortion parameters reduces to M distinct optimization processes, while *Joint* corresponds to a global optimization process. Further, minimizing each $E[C(\boldsymbol{w}_m(n))]$ separately is not equivalent to minimizing the global cost $E[C(\boldsymbol{w}_1(n), \ldots, \boldsymbol{w}_M(n))]$.

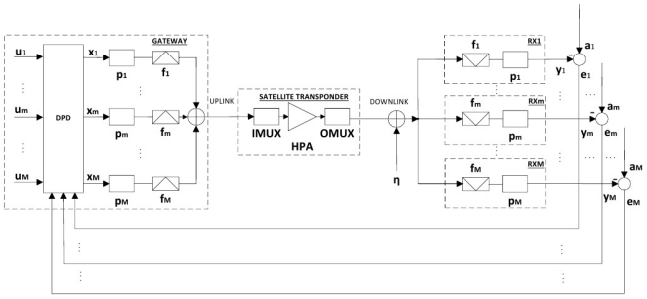

Fig. 4. Pre-inverse Channel Estimation

Unlike the indirect approach, the direct estimation cannot be formulated as a standard least squares problem [12]. As a consequence, it can only be implemented through iterative techniques. We now elaborate the iterative formulations for the direct estimation where the well known LMS and RLS are considered with some modifications.

B. Individual Predistorter Design

In this section, we develop first order techniques aimed at minimizing the error $E[|e_m(n)|^2]$, separately on each carrier, with respect to its corresponding predistortion coefficients $\boldsymbol{w}_m$ (kindly refer to Fig. 5). These algorithms approximate

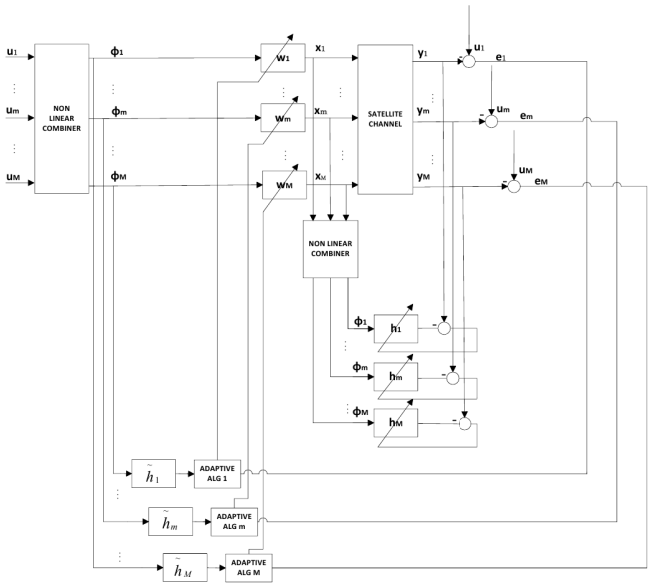

Fig. 5. Functional scheme describing the individual direct estimation method

$E[|e_m(n)|^2]$ and provide an iterative approach towards the solution. The simpler LMS algorithm is presented first followed by the RLS technique that yields superior performance at the cost of added complexity.

1) LMS Formulation: In the standard LMS algorithm, we consider the instantaneous error magnitude, $C_m(\boldsymbol{w}_m(n))$, as the cost function. Thus, in the pursued iterative optimization solution, the predistorter coefficients are updated as,

$$\boldsymbol{w}_m(n+1) = \boldsymbol{w}_m(n) + \frac{\mu}{2} \frac{\partial C_m(\boldsymbol{w}_m(n))}{\partial \boldsymbol{w}_m(n)}. \tag{21}$$

In (21), the iteration index is explicitly depicted and we will continue to do so when dealing with updates of the predistorter coefficients. Since $C_m(\boldsymbol{w}_m(n)) = |e_m(n)|^2$, (21) can be approximated to,

$$\boldsymbol{w}_m(n+1) = \boldsymbol{w}_m(n) + \mu e_m^*(n) \frac{\partial y_m(n)}{\partial \boldsymbol{w}_m(n)}. \tag{22}$$

Similarly to [12], we define the Instantaneous Equivalent Filter (IEF) relative to carrier m as,

$$\tilde{h}_m(n,l) = \frac{\partial y_m(n)}{\partial x_m(n-l)} \tag{23}$$

The IEL can be analytically extracted using (16) as,

$$\tilde{h}_m(n,l) = \boldsymbol{h}_m^T \frac{\partial \boldsymbol{\phi}_m(\boldsymbol{x}(n))}{\partial x_m(n-l)}, \tag{24}$$

where computation of the entries of $\frac{\partial \boldsymbol{\phi}_m(\boldsymbol{x}(n))}{\partial x_m(n-l)}$ is based on the application of the partial differential rules defined in [21] to multicarrier complex polynomial functions (kindly refer to

Appendix A). The gradient $\frac{\partial y_m(n)}{\partial \boldsymbol{w}_m(n)}$ can be expressed using the channel differentiability and the chain rule as,

$$\frac{\partial y_m(n)}{\partial \boldsymbol{w}_m(n)} = \sum_{l=-K}^{K} \tilde{h}_m(n,l) \frac{\partial x_m(n-l)}{\partial \boldsymbol{w}_m(n)}. \tag{25}$$

Recalling $x_m(n-l) = \boldsymbol{w}_m^T(n-l)\left[\boldsymbol{\phi}_m(\boldsymbol{u}(n-l))\right]$ from (15), and approximating $\boldsymbol{w}_m(n) \approx \boldsymbol{w}_m(n-l)$ within memory range (similarly to [12]), we obtain,

$$\frac{\partial x_m(n-l)}{\partial \boldsymbol{w}_m(n)} \approx \boldsymbol{\phi}_m(\boldsymbol{u}(n-l)). \tag{26}$$

Using (26) and (24) in (25), we have,

$$\frac{\partial y_m(n)}{\partial \boldsymbol{w}_m(n)} = \sum_{l=-K}^{K} \tilde{h}_m(n,l) \boldsymbol{\phi}_m(\boldsymbol{u}(n-l)) \tag{27}$$

Equation (27) together with (22) provides the LMS step for the optimization. Notice that each vector $\boldsymbol{w}_m(n)$ is initialized such that the resulting predistortion functions simply correspond to $x_m(n) = u_m(n), \forall\ m$. As an example, if $K_d = 0, \forall d$ (no memory), then $\boldsymbol{w}_m(0)$ corresponds to the mth standard basis of dimension $\sum_p |\Omega_{m,p}| \times 1$.

2) RLS Formulation: For each carrier m, we now minimize $C_m(\boldsymbol{w}_m(n)) = \sum_{i=1}^{n} \lambda^{n-i} |e_m(i)|^2$ with respect to the corresponding $\boldsymbol{w}_m(n)$. The choice of the forgetting factor λ affects the performance and will be discussed in the simulation section. As a first step towards defining the RLS, we set,

$$-2\sum_{i=1}^{n} \lambda^{n-i} \frac{\partial y_m(i)}{\partial \boldsymbol{w}_m(n)} e_m^*(i) = \mathbf{0}. \tag{28}$$

Similarly to [12], we use the weak non-linearity assumption to approximate the instantaneous channel output as,

$$y_m(n) \approx \sum_{l=-K}^{K} \tilde{h}_m(n,l) x_m(n-l). \tag{29}$$

Referring to Appendix B and using (29), we arrive at the following standard formulation for (28),

$$\begin{aligned} \mathbf{R}_m(n)\boldsymbol{w}_m(n) &= \boldsymbol{r}_m(n), \quad \text{where} \\ \mathbf{R}_m(n) &= \sum_{i=1}^{n} \lambda^{n-i} \left[\frac{\partial y_m(i)}{\partial \boldsymbol{w}_m(n)}\right]^* \left[\frac{\partial y_m(i)}{\partial \boldsymbol{w}_m(n)}\right]^T, \\ \boldsymbol{r}_m(n) &= \sum_{i=1}^{n} \lambda^{n-i} \left[\frac{\partial y_m(i)}{\partial \boldsymbol{w}_m(n)}\right]^* \boldsymbol{u}_m(i). \end{aligned} \tag{30}$$

The formulation in (30) is amenable to a RLS implementation involving the following updates,

$$\boldsymbol{w}_m(n+1) = \boldsymbol{w}_m(n) + \mu \boldsymbol{k}_m(n) e_m(n), \tag{31}$$

where the gain vector $\boldsymbol{k}_m$ is obtained from,

$$\boldsymbol{k}_m(n) = \frac{\lambda^{-1}\mathbf{P}_m(n-1)\left[\frac{\partial y_m(n)}{\partial \boldsymbol{w}_m(n)}\right]}{1 + \lambda^{-1}\left[\frac{\partial y_m(n)}{\partial \boldsymbol{w}_m(n)}\right]^H \mathbf{P}_m(n-1)\left[\frac{\partial y_m(n)}{\partial \boldsymbol{w}_m(n)}\right]}, \tag{32}$$

and the positive semidefinite matrix $\mathbf{P}_m$ satisfies the recursive relation,

$$\mathbf{P}_m(n) = \lambda^{-1}(\mathbf{P}_m(n-1) - \boldsymbol{k}_m(n)\left[\frac{\partial y_m(n)}{\partial \boldsymbol{w}_m(n)}\right]^H \mathbf{P}_m(n-1)). \tag{33}$$

Notice that, we choose $\mathbf{P}_m(0) = \mathbf{I}$ and $\boldsymbol{w}_m(n)$ is initialized as in Section IV-B1. Further note that the evaluation of $\frac{\partial y_m(n)}{\partial \boldsymbol{w}_m(n)}$ follows from Section IV-B1.

The individual estimation method results in M independent optimization processes to be run in parallel generating M predistortion coefficients vector $\{\mathbf{w}_m\}$. In the following section, we pursue a completely different approach where all predistortion parameters are estimated jointly towards achieving a global optimum.

C. Joint Predistorter Design

Each channel output $y_m(n)$ is a function of the predistorted symbols $\boldsymbol{x}(n)$ from all M input carriers as defined in (16). Intuitively, this calls for a joint estimation of the predistorter coefficients $\boldsymbol{w}_m$. In this section we develop first order techniques aimed to minimize the cost function $E[\sum_{m=1}^{M} |e_m(n)|^2]$ with respect to the predistortion coefficients of all the M carriers, compactly defined here defined as,

$$\boldsymbol{w} = [\boldsymbol{w}_1^T, \ldots, \boldsymbol{w}_M^T]^T. \tag{34}$$

In Fig. 6 the scheme of the joint estimation method is illustrated. As mentioned earlier, joint estimation of $\{\boldsymbol{w}_m\}$

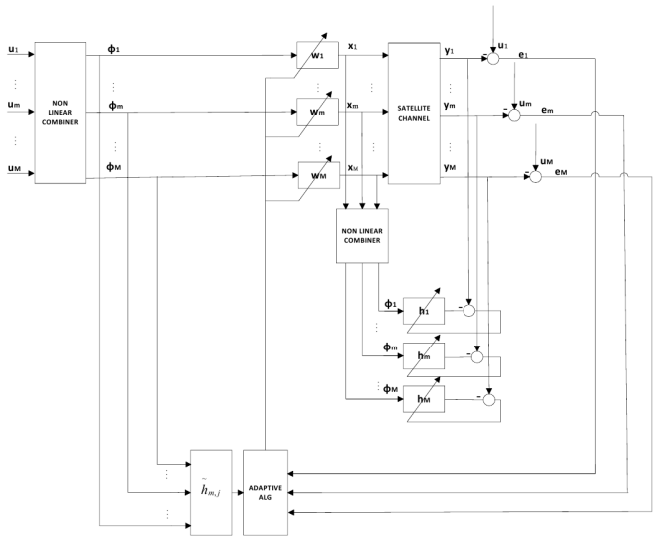

Fig. 6. Functional scheme describing the joint direct estimation method

is not a generalization of the individual optimization method described in Section IV-B. The joint estimation methodology exploits the interdependence between channel outputs $y_m(n)$ and kernel coefficients $\boldsymbol{w}_i(n), i \neq m$. This results in an improved performance compared to the individual estimation, but at the cost of higher complexity.

1) LMS Formulation: The standard LMS formulation for this problem can be written similarly to (21). With $C(\boldsymbol{w}(n)) = \sum_{m=1}^{M} |e_m(n)|^2$, we use the update equation,

$$\boldsymbol{w}(n+1) = \boldsymbol{w}(n) + \mu \sum_{m=1}^{M} \frac{\partial y_m(n)}{\partial \boldsymbol{w}(n)} e_m^*(n). \tag{35}$$

Based on form of $\boldsymbol{w}$ described in (34), we define the $\sum_m \sum_p (2K_p + 1)|\Omega_{m,p}| \times 1$ dimensional column vector $\frac{\partial y_m(n)}{\partial \boldsymbol{w}(n)}$ as,

$$\frac{\partial y_m(n)}{\partial \boldsymbol{w}(n)} = \left[\frac{\partial y_m(n)}{\partial \boldsymbol{w}_1(n)}^T \cdots \frac{\partial y_m(n)}{\partial \boldsymbol{w}_M(n)}^T \right]^T. \quad (36)$$

Notice the complexity increase required for the computation of terms $\{\frac{\partial y_m(n)}{\partial \boldsymbol{w}(n)}\}_{m=1}^M$ in (36) compared to the individual LMS estimation in (22) where only terms $\{\frac{\partial y_m(n)}{\partial \boldsymbol{w}_m(n)}\}_{m=1}^M$ are required.

Similarly to [12], we define the Instantaneous Equivalent Filter (IEF) relative to carrier m with respect to carrier j as,

$$\tilde{h}_{m,j}(n,l) = \frac{\partial y_m(n)}{\partial x_j(n-l)} \quad (37)$$

Note, that unlike in (23) of Section IV-B1, we include here two subscripts for carrier m and j, respectively. Further, similar to (26), we have,

$$\tilde{h}_{m,j}(n,l) = \boldsymbol{h}_m^T \frac{\partial \boldsymbol{\phi}_m(\boldsymbol{x}(n))}{\partial x_j(n-l)}. \quad (38)$$

In (38), the entries of $\frac{\partial \boldsymbol{\phi}_m(\boldsymbol{x}(n))}{\partial x_j(n-l)}$ are computed based on the partial differential rules defined in [21] elaborated to the case of multicarrier complex polynomial functions (kindly refer to Appendix A). Each differential vector $\frac{\partial y_m(n)}{\partial \boldsymbol{w}_j(n)}$ in (36) can be expressed exploiting channel differentiability and the chain rule as,

$$\frac{\partial y_m(n)}{\partial \boldsymbol{w}_j(n)} = \sum_{l=-K}^{K} \tilde{h}_{m,j}(n,l) \frac{\partial x_j(n-l)}{\partial \boldsymbol{w}_j(n)}, \quad (39)$$

where

$$\frac{\partial x_j(n-l)}{\partial \boldsymbol{w}_j(n)} \approx \boldsymbol{\phi}_m(\boldsymbol{u}(n-l)). \quad (40)$$

Using (40) and (38) in (39), we finally obtain an expression for the gradient as,

$$\frac{\partial y_m(n)}{\partial \boldsymbol{w}_j(n)} = \sum_{l=-K}^{K} \tilde{h}_{m,j}(n,l) \boldsymbol{\phi}_m(\boldsymbol{u}(n-l)). \quad (41)$$

Equations (41) and (36) together with (35) provide the LMS step for the optimization.It should be noted that, even in this case, the individual vectors $\boldsymbol{w}_m(0)$ are initialized as in Section IV-B1 and the global vector $\boldsymbol{w}(0)$ obtained from (34).

2) RLS Formulation: The objective function to be minimized with respect to the overall predistortion coefficients vector $\boldsymbol{w}$ defined in (34) takes the form $C(\boldsymbol{w}(n)) = \sum_{j=1}^{M} \sum_{i=1}^{n} \lambda^{n-i} |e_j(i)|^2$ where λ is the forgetting factor. To proceed with the analysis, we introduce,

$$\boldsymbol{e}(n) = [e_1(n), \ldots, e_M(n)]^T \quad (42)$$

$$\frac{\partial \boldsymbol{y}(i)}{\partial \boldsymbol{w}(n)} = \left[\frac{\partial y_1(i)}{\partial \boldsymbol{w}(n)}, \ldots, \frac{\partial y_M(i)}{\partial \boldsymbol{w}(n)} \right] \quad (43)$$

where $\frac{\partial \boldsymbol{y}(i)}{\partial \boldsymbol{w}(n)}$ is $\sum_m \sum_p |\Omega_{m,p}| \times M$ matrix and $\frac{\partial y_m(i)}{\partial \boldsymbol{w}(n)}$ is obtained from (36). Notice in (43), as with the joint LMS formulation of Section IV-C1, we can identify a complexity increase with respect to the individual RLS estimation in (28) where only terms $\{\frac{\partial y_m(n)}{\partial \boldsymbol{w}_m(n)}\}_{m=1}^M$ are required.

Towards defining the global RLS, we set,

$$-2 \sum_{i=1}^{n} \lambda^{n-i} \frac{\partial \boldsymbol{y}(i)}{\partial \boldsymbol{w}(n)} \boldsymbol{e}^*(i) = \boldsymbol{0}. \quad (44)$$

Similarly to [12], we use the weak non-linearity assumption to approximate the instantaneous channel output as,

$$y_m(n) \approx \sum_{l=-K}^{K} \sum_{j=1}^{M} \tilde{h}_{m,j}(n,l) x_j(n-l). \quad (45)$$

Referring to Appendix C, the weak non-linearity approximation of (45), and using the definition in (43), we obtain for (44) a recursive solution:

$$\begin{aligned} \mathbf{R}(n)\boldsymbol{w}(n) &= \boldsymbol{r}(n), \quad (46) \\ \mathbf{R}(n) &= \sum_{i=1}^{n} \lambda^{n-i} \left[\frac{\partial \boldsymbol{y}(i)}{\partial \boldsymbol{w}(n)} \right]^* \left[\frac{\partial \boldsymbol{y}(i)}{\partial \boldsymbol{w}(n)} \right]^T \\ \boldsymbol{r}(n) &= \sum_{i=1}^{n} \lambda^{n-i} \left[\frac{\partial \boldsymbol{y}(i)}{\partial \boldsymbol{w}(n)} \right]^* \boldsymbol{u}(i) \end{aligned}$$

This leads to the following recursive set of equations,

$$\boldsymbol{w}(n+1) = \boldsymbol{w}(n) + \mu \mathbf{K}(n) \boldsymbol{e}(n), \quad (47)$$

$$\begin{aligned} \mathbf{K}(n) = \lambda^{-1} \mathbf{P}(n-1) \frac{\partial \boldsymbol{y}(n)}{\partial \boldsymbol{w}(n)} \times \\ (\mathbf{I} + \lambda^{-1} \left[\frac{\partial \boldsymbol{y}(n)}{\partial \boldsymbol{w}(n)} \right]^H \mathbf{P}(n-1) \frac{\partial \boldsymbol{y}(n)}{\partial \boldsymbol{w}(n)})^{-1}, \end{aligned}$$

$$\mathbf{P}(n) = \lambda^{-1} (\mathbf{P}(n-1) - \mathbf{K}(n) \left[\frac{\partial \boldsymbol{y}(n)}{\partial \boldsymbol{w}(n)} \right]^H \mathbf{P}(n-1)). \quad (48)$$

Unlike in Section IV-B2, we now deal with a $\sum_m \sum_p |\Omega_{m,p}| \times M$ gain matrix $\mathbf{K}(n)$ in the update equations. Notice that $\mathbf{P}(0) = \mathbf{I}$ and $\boldsymbol{w}(0)$ is initialized as in the earlier section.

V. Simulation Results

In the following, we compare the performance of the proposed direct estimation method for a multicarrier memory polynomial predistorter with respect to the known indirect approach. Through extensive numerical simulations covering several scenarios, we evaluate the gain obtained by the proposed approach. Such an evaluation combines both power efficiency and error performance, since the two quantities are typically in conflict.

A. Figure of Merit

Total Degradation is a standard figure of merit for evaluating the performance over non-linear channels [2], [5]. It is defined as,

$$TD|_{@BER} = \frac{E_s}{N_0}|_{NL} - \frac{E_s}{N_0}|_{AWGN} + OBO \quad (49)$$

where $\frac{E_s}{N_0}|_{NL} - \frac{E_s}{N_0}|_{AWGN}$ represents the energy loss between the non-linear and linear channels for a given target bit error rate (BER). OBO is defined as the ratio in dB between the multicarrier signal output power and the saturation output

power of the selected amplifier model. For the considered amplifier model we have a nominal saturation output power of 0 dB. When the amplifier is operated in high efficiency region it yields strong distortion effects increasing the needed $\frac{E_s}{N_0}|_{NL}$, while in linear operation we have a power efficiency degradation accounted by the measure of OBO. The total degradation is illustrated as a function of the OBO resulting in a convex curve whose minimum identifies the optimal amplifier operating point. Notice that (49) reduces to $TD|_{@BER} = OBO$ in case of perfect compensation or absence of non-linear interference and serves as a lower bound.

B. Set Up

Referring to Fig. 1, we consider two channel scenarios with three and five equally spaced carriers, respectively. Spectrally efficient modulation schemes are applied in each carrier channel. The set of channel parameters are summarized in Table I. In Table I, the DPD parameter estimation noise

TABLE I
SIMULATION PARAMETERS

Number of carriers	$M_c = 3,\ 5$
Symbols rate, Roll Off	$R_s = 8$ MBaud, $\rho = 0.25$
Carrier frequency spacing, $\triangle f$	1.25 R_s
Modulation, Coderate (LDPC)	16 APSK, 2/3
Target BER	10^{-5}
$\frac{E_s}{N_0}\|_{AWGN}$ @ Target BER	9.05 dB
DPD parameter estimation noise	$\frac{E_s}{N_0} = 9.05$ dB
HPA	Saleh model [19]
Channel filters IMUX /OMUX	$BW_{1dB} \approx\ M\ R_s(1+\rho)$
Oversampling factor	20

corresponds to the receiver $\frac{E_s}{N_0}$ set during the estimation of the kernel parameter for all the considered techniques. A high oversampling is needed for simulating the chain due to the spectral enlargement caused by non-linearities.

C. Predistortion Structure

In order to have a fair comparison among the different parameter estimation techniques, the structure and complexity of the underlying predistortion function is kept the same. Moreover 10000 training symbols are used in all the techniques. This allows us to identify the gains obtained from better parameter estimation. In particular, the memory polynomial model defined in (15) is used with a memory depth of three ($K_d = 1, \forall d$) and polynomial degree of three ($d = 3$). Table II provides the frequency-centered intermodulation products $\Omega_{m,d}$ derived in [3] and included in the predistorter evaluation for the three and five carriers scenarios, respectively. With the considered memory, degree and interfering carriers, it can be shown that the number of predistorter coefficients are 63 and 207 for the three and five carrier, respectively.

D. Convergence Performance

Central to the performance of direct estimation techniques is the determination of the adaptation parameters (μ, λ) that

TABLE II
FREQUANCY CENTERED IMD [3]: (A) THREE CARRIER CHANNEL IN-BAND TERMS, (B) FIVE CARRIERS CHANNEL IN-BAND TERMS

(A)

$\Omega_{1,3}$	$\Omega_{2,3}$	$\Omega_{3,3}$
[111]	[121]	[131]
[122]	[132]	[221]
[133]	[222]	[232]
[223]	[233]	[333]

(B)

$\Omega_{1,3}$	$\Omega_{2,3}$	$\Omega_{3,3}$	$\Omega_{4,3}$	$\Omega_{5,3}$
[111]	[121]	[131]	[141]	[151]
[122]	[132]	[142]	[152]	[241]
[133]	[143]	[153]	[231]	[252]
[144]	[154]	[221]	[242]	[331]
[155]	[222]	[232]	[253]	[342]
[223]	[233]	[243]	[332]	[353]
[234]	[244]	[254]	[343]	[443]
[245]	[255]	[333]	[354]	[454]
[335]	[334]	[344]	[444]	[555]
[-]	[345]	[355]	[455]	[-]
[-]	[-]	[445]	[-]	[-]

guarantee fast convergence. Similarly to [12], [20], this is achieved by fine tuning of the adaptation parameters. In both the Individual and Joint methods, the parameters μ and λ have been tuned to provide minimal residual error. For the LMS updates of (22) and (35) we set $\mu = 0.00001$, while for the RLS updates defined in (31) and (47), we set $\mu = 0.005$ and $\lambda = 0.95$. In Figs. 7 and 8 we show the envelope of the squared error $|e_m(n)|^2$ for the individual and joint techniques, respectively. The plotted envelopes relate to the central carrier in the three carriers scenario. These curves indicate that the simpler LMS algorithm performs poorly compared to RLS in terms of convergence performance. Hence, we focus on direct estimation techniques implemented using the described RLS algorithms. This result is consistent with [3], where the LMS and RLS techniques were developed for the estimation of the IMD in a multicarrier scenario and the suitability of RLS over LMS was also illustrated.

E. Total Degradation Results

We evaluate TD for the considered scenarios. For $M = 3$ equally spaced carriers, Figures 9 and 10 respectively present the TD for the central and external carriers. The results for the external carriers are symmetric and hence only one is reported. As expected, significant degradation occurs in the central carrier due to the stronger ACI. Multicarrier predistortion, in general, provides significant gains (> 3 dB) with respect to a baseline scenario where no compensation applied (legend *No Compensation* in Fig. 9). Direct estimation of the predistorter parameters provides further gain over the indirect estimation. The joint optimization method yields the best performance providing about $0.5 - 1$dB gain over the indirect method for the same predistorter complexity and training length.

To the best of authors' knowledge, there exist no published work on multicarrier techniques for a direct comparison. A related work, that tackles a similar scenario (same HPA model, modulation, coderate, roll off and frequency spacing) but using a multicarrier equalizer (instead of predistortion) coupled with turbo decoder can be found in [3]. Further, unlike our case, [3] does not consider on-board channelization filters (IMUX and

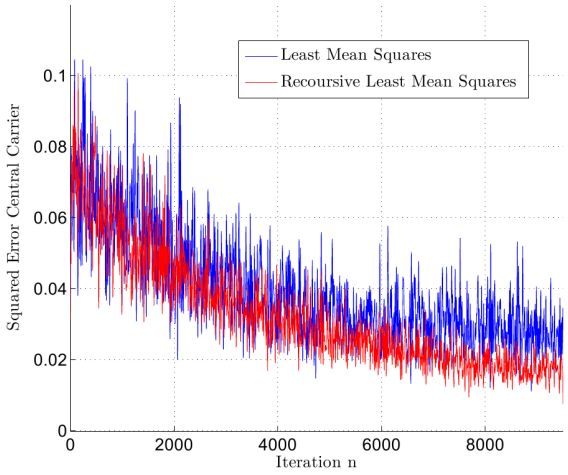

Fig. 7. Direct Individual Method Convergence:Central Carrier with $M = 3$

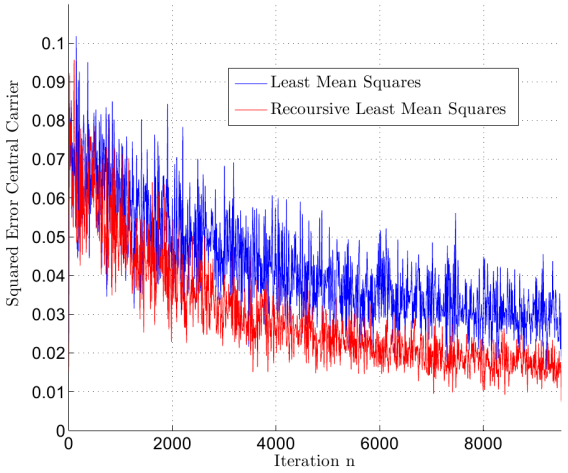

Fig. 8. Direct Joint Method Convergence:Central Carrier with $M = 3$

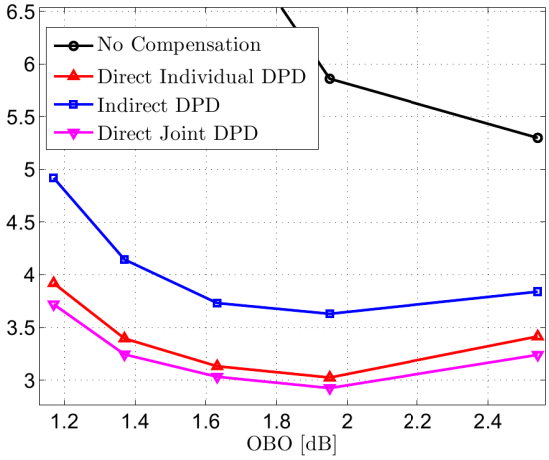

Fig. 9. Total Degradation of the central carrier in a three carrier scenario

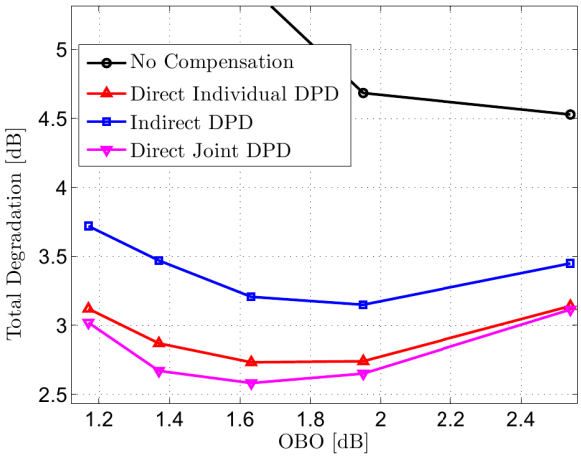

Fig. 10. Total Degradation of the external carrier in a three carrier scenario

OMUX). These dissimilarities not withstanding, we consider Fig. 4 of [3] with Fig. 9 above. Figure 4 in [3] depicts the BER of the central carrier for an OBO = 2.1 dB that corresponds to a total degradation of $2.75 - 3$ dB depending on the specific configuration in place. This value is very similar to those achieved by our joint predistortion solution ($TD \approx 3$ dB in Fig. 9).

TD results for a five carrier satellite channel are provided in Figs. 11, 12, 13 for the carriers located at center, immediate left to the center and leftmost locations. Compared to the three carrier scenario the degradation is prominent. In this very challenging configuration, the advantage of the direct optimization methods over the indirect one is still valuable providing additional $0.5 - 0.75$dB of gain.

F. Estimation Noise Sensitivity Analysis

We now investigate the robustness of the proposed direct estimation methods to the estimation noise. The estimation noise is defined as the ambient noise level at the receiver during the predistorter parameter estimation. In the considered scenario, the estimation of the predistorter parameters takes place off-line with the support of a dedicated user terminal in charge of providing feedback to the transmitting GW. The noise level at the considered receiver plays a key role in the estimation accuracy of the predistorter parameter and in determining the final system performance.

Fig. 14 illustrates the normalized noiseless interference level, defined as $E[|u_m(n) - y_m(n)|^2]/E[|y_m(n)|^2]$, with respect to the estimation noise level $\frac{E_s}{N_0}$ for the three carrier scenario. This result indicates that the indirect estimation is very sensitive to the noise level. On the other hand, direct estimation is robust and provides improved performance. This is consistent with the results for single carrier signal predistortion provided in [18]. Joint direct estimation is shown to guarantee the best performance independently of the estimation noise level. This allows the system designer to employ a predistorter over a wider range of $\frac{E_s}{N_0}$, thereby reducing the operational costs.

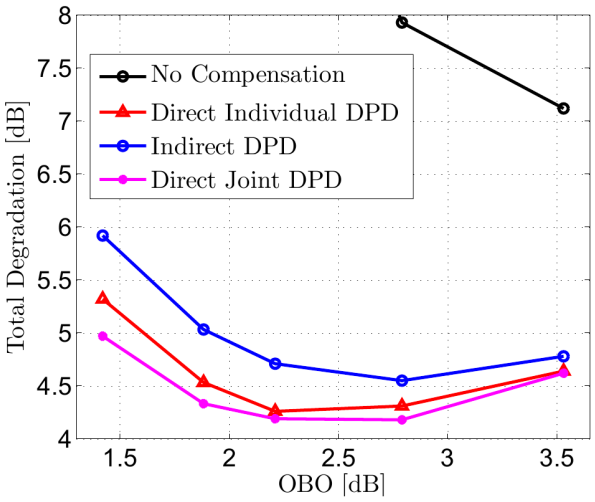

Fig. 11. Consider Total Degradation of the center carrier in a five carriers scenario

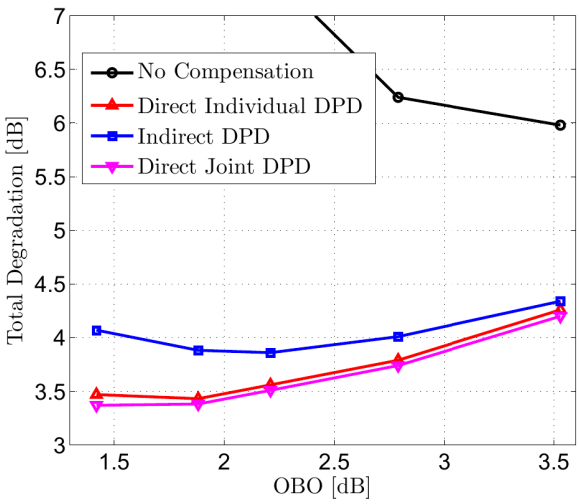

Fig. 13. Total Degradation of the leftmost carrier in a five carriers scenario

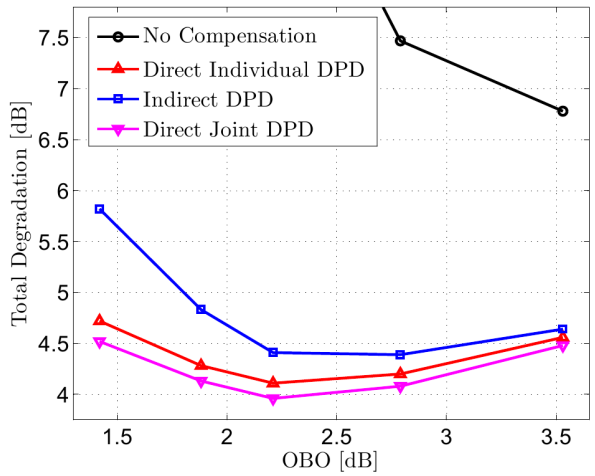

Fig. 12. Total Degradation of the left to the center carrier in a five carrier scenario

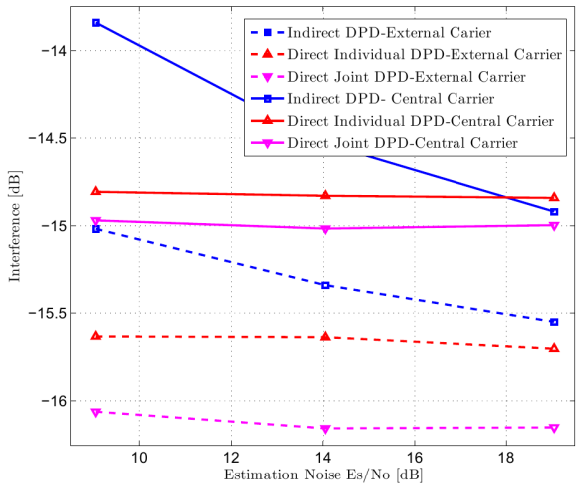

Fig. 14. Three Carriers: Estimation noise vs Interference (OBO = 1.7 dB)

G. *Sensitivity to Mismatched Estimation*

In this section, we evaluate the sensitivity of the system performance to mismatches in scenarios: between the one prevailing during the estimation of predistortion coefficients and the one when the predistortion is in operation. Slight differences in the processing of the individual carriers, can arise out of the system components (cables/ waveguide lengths), on-ground amplifier settings, feedback delay and propagation conditions. We consider two prominent manifestations of these differences: power imbalance and timing misalignments among the carriers.

Sensitivity of different predistortion techniques to power imbalance is assessed by forcing different carrier power levels on the down link channel during the predistorter estimation; on the other hand, the performance is evaluated with identical down link power on all carriers. In Fig. 15 we depict the variation in TD with power imbalance for a three carrier scenario. In particular, the imbalance is defined as the ratio between the signal power of the external carriers (both having the identical power levels for simplicity) and the signal power of the central carrier. Performance of the central carrier is sensitive to the power imbalance only in the case of indirect estimation (about 20% variation) while only a minor degradation is observed in the cases of individual and joint direct estimation (kindly refer to Fig. 15). The external carriers are rather robust to power imbalance for all estimation methodologies, even exhibiting minor improvements. The minor improvement in the external carriers can be related to the magnitude of the predistortion parameters of the central carrier. In fact, due to the lower signal to noise ratio (in case of power imbalance) of the central carrier during estimation, the related predistortion parameters show a lower magnitude compared to the external ones. This magnitude imbalance in the predistortion function slightly reduces the uplink power of the central carrier, thereby

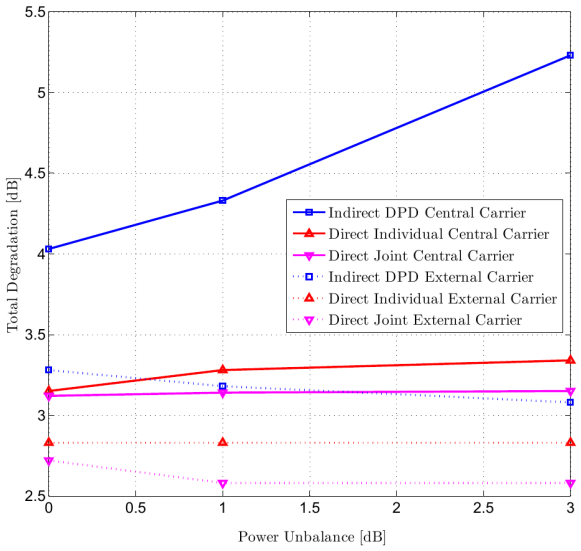

Fig. 15. Sensitivity of TD to power imbalance of central carrier during estimation: Three carrier scenario (OBO = 1.3 dB)

lowering the corresponding ACI injected onto the external carriers.

Similar to the power imbalance case, we consider predistorter parameters estimation with some timing misalignment during uplink process, while performance is assessed in the case of perfect matching using the TD . We considered a three carrier scenario where the two external carriers are perfectly aligned, while the central carrier has a timing misalignment defined as a percentage of the symbols time T_s. The external carriers experience minor variation with respect to this misalignment while the central carrier suffers performance degradation for all considered methodologies (kindly refer to Fig 16). Joint estimation is shown to be less sensitive to

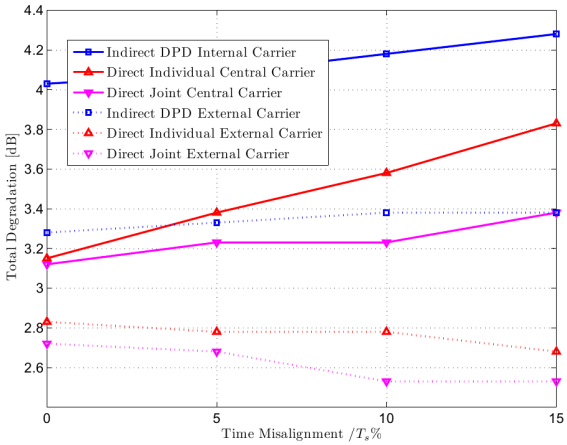

Fig. 16. Sensitivity of TD to timing misalignment of central carrier during estimation: Three carrier scenario (OBO = 1.3 dB)

timing errors with respect to the other techniques; further direct individual estimation is more sensitive than indirect estimation. Notice in this case that direct techniques show a very minor improvement in the external carriers

H. Complexity Discussion

Direct estimation, while providing for increased performance, requires additional complexity compared to indirect estimation. Direct estimation relies on the knowledge of the channel parameters that need to be estimated in the adaptation loop, while indirect estimation does not require the channel parameters. This does not increase the amount of data feedback required to the gateway but the complexity of the processing. Further, individual direct estimation has a lower complexity compared to the joint one in the number of parameters computed. The complexity of individual and joint predistortion techniques can be compared considering the number of scalar differential terms of the kind $\frac{\partial y_m}{\partial w_{i,j}}$ that are computed at each iteration. This number is the same for both LMS and RLS implementations. For individual predistortion, considering all the M carriers, we require the computation of $\sum_m \sum_p (2K_p + 1)|\Omega_{m,p}|$ differential terms (kindly refer to (22)). On the other hand for joint predistortion $M \sum_m \sum_p (2K_p + 1)|\Omega_{m,p}|$ differential terms are required (kindly refer to (35)).

VI. Conclusions

This paper proposes two novel techniques for multicarrier predistorter design in a non-linear satellite channel. Implemented through iterative first order techniques, these estimation methods, namely *Individual* and *Joint* DPD, provide optimized model parameters for a memory polynomial based predistorter. The individual DPD method optimizes the predistortier coefficients for different carriers separately, while the joint method favors a global optimization of the coefficients at the cost of increased complexity. Through simulations we have shown that the direct estimation of parameters provides improved performance over the well-known indirect estimation method, achieving gains that are valuable in the satellite context. Direct estimation also leads to a predistorter that is robust to the level of noise present during the estimation and to channel mismatch. Depending on the complexity affordable, either the *Joint* or the *Individual* method could serve as a promising technique for the current and future satellite missions where power and spectral efficiencies play a vital role.

Appendix A
Partial Derivates Formulation

As proposed in [21], we assume x and x^* to be independent variables while differentiating a complex polynomial. Based on this, we can derive some basic differentiation rules for multicarrier complex polynomial functions as,

$$\frac{\partial (x_m |x_m|^{2P})}{\partial x_m} = (P+1)|x_m|^{2P} \tag{50}$$

$$\frac{\partial (x_j |x_m|^{2P})}{\partial x_j} = |x_m|^{2P} \tag{51}$$

$$\frac{\partial (x_j |x_m|^{2P})}{\partial x_m} = P x_j x_m^* |x_m|^{2(P-1)} \tag{52}$$

Since the entries of $\boldsymbol{\phi}_m(\boldsymbol{x}(i))$ take the form in (8), we can exploit the aforementioned rules to generate quantities of the form $\frac{\partial \boldsymbol{\phi}_m(\boldsymbol{x}(n))}{\partial x_m(n-l)}$.

APPENDIX B
RLS DERIVATION FOR INDIVIDUAL PREDISTORTER DESIGN

Similar to [12], we approximate $e_m(i)$ exploiting the differentiability of the channel. Using the the weak non-linearity approximation of (29) and recalling $x_m(i-l) \approx [\boldsymbol{\phi}_m(\boldsymbol{u}(i-l))]^T \boldsymbol{w}_m(n)$ from Section IV-B1 we have,

$$y_m(i) \approx \left(\sum_{l=-K}^{K} \tilde{h}_m(i,l) \boldsymbol{\phi}_m(\boldsymbol{u}(i-l)) \right)^T \boldsymbol{w}_m(n). \quad (53)$$

Using (53) and recalling (24), (27), we can express the error as,

$$e_m(i) \approx u_m(i) - \left[\frac{\partial y_m(i)}{\partial \boldsymbol{w}_m(n)} \right]^T \boldsymbol{w}_m(n) \quad (54)$$

This simplified expression (54) can be used in (28) to transform the problem to standard RLS formulation.

APPENDIX C
RLS DERIVATION FOR JOINT PREDISTORTER DESIGN

Similarly to the derivation carried out in the earlier section, we use the weak non-linearity approximation of (45) and recalling $x_m(i-l) \approx [\boldsymbol{\phi}_m(\boldsymbol{u}(i-l))]^T \boldsymbol{w}_m(n)$ to derive,

$$y_j(i) \approx \left(\sum_{m=1}^{M} \sum_{l=-K}^{K} \tilde{h}_{j,m}(n,l) \left[\boldsymbol{\phi}_m(\boldsymbol{u}(i-l)) \right] \right)^T \boldsymbol{w}_m(n).$$

Using (55) and recalling (24), (41) we can express the error as

$$e_j(i) \approx u_j(i) - \left[\frac{\partial y_j(i)}{\partial \boldsymbol{w}(n)} \right]^T \boldsymbol{w}(n) \quad (55)$$

This simplified expression (55) can be used in (44) to transform the problem in a standard RLS problem.

REFERENCES

[1] S. Benedetto and E. Biglieri, "Nonlinear equalization of digital satellite channels," *IEEE J. Sel. Areas Commun.*, vol. 1, pp. 57 –62, Jan. 1983.

[2] B. F. Beidas and R. Seshadri, "Analysis and compensation for nonlinear interference of two high-order modulation carriers over satellite link," *IEEE Trans. Commun.*, vol. 58, no. 6, pp. 1824 –1833, June 2010.

[3] B. F. Beidas, "Intermodulation distortion in multicarrier satellite systems: Analysis and turbo volterra equalization," *IEEE Trans. Commun.*, vol. 59, no. 6, pp. 1580 –1590, June 2011.

[4] G. E. Corazza, *Digital Satellite Communications, Chapter 8*. Springer, 2007.

[5] E. Casini, R. De Gaudenzi, and A. Ginesi, "DVB- S2 modem algorithms design and performance over typical satellite channels," *Intern. J.on Satellite Commun. and Networking*, vol. 22, pp. 281–318, 2004.

[6] G. Karam and H. Sari, "A data predistortion technique with memory for QAM radio systems," *IEEE Trans. Commun.*, vol. 39, no. 2, pp. 336 –344, Feb 1991.

[7] M. Schetzen, *The Volterra and Wiener Theories of Nonlinear Systems*. John Wiley & Sons, Apr. 1980. [Online]. Available: http://www.worldcat.org/isbn/0471044555

[8] C. Eun and E. Powers, "A new volterra predistorter based on the indirect learning architecture," *Signal Processing, IEEE Trans. on*, vol. 45, no. 1, pp. 223 –227, Jan 1997.

[9] L. Ding, R. Raich, and G. T. Zhou, "A hammerstein predistortion linearization design based on the indirect learning architecture," in *Acoustics, Speech, and Signal Processing (ICASSP), 2002 IEEE International Conference on*, vol. 3, May 2002, pp. III–2689 –III–2692.

[10] C. Sheng, "An efficient predistorter design for compensating nonlinear memory high power amplifiers," *IEEE Trans. Broadcast.*, vol. 57, no. 4, pp. 856 –865, Dec. 2011.

[11] L. Ding, G. T. Zhou, D. R. Morgan, Z. Ma, J. S. Kenney, J. Kim, and C. R. Giardina, "A robust digital baseband predistorter constructed using memory polynomials," *IEEE Trans. Commun.*, vol. 52, no. 1, pp. 159 – 165, Jan. 2004.

[12] D. Zhou and V. E. DeBrunner, "Novel adaptive nonlinear predistorters based on the direct learning algorithm," *Signal Processing, IEEE Transactions on*, vol. 55, no. 1, pp. 120 –133, Jan. 2007.

[13] M. Y. Cheong, S. Werner, M. Bruno, J. Figueroa, J. Cousseau, and R. Wichman, "Adaptive piecewise linear predistorters for nonlinear power amplifiers with memory," *Circuits and Systems I: Regular Papers, IEEE Transactions on*, vol. 59, no. 7, pp. 1519–1532, July 2012.

[14] R. Piazza, B. Shankar, and B. Ottersten, "Non-parametric data predistortion for non-linear channels with memory," in *Acoustics, Speech, and Signal Processing (ICASSP), 2013 IEEE International Conference on*. [Online]. Available: http://orbilu.uni.lu/handle/10993/4862

[15] S. Bassam, M. Helaoui, and F. Ghannouchi, "2-D digital predistortion (2-D-DPD) architecture for concurrent dual-band transmitters," *Microw. Theory and Techniques, IEEE Trans. on*, vol. 59, no. 10, pp. 2547 –2553, Oct. 2011.

[16] R. Piazza, E. Zenteno, and e. al, "Multicarrier digital predistortion/ equalization techniques for non-linear satellite channels," in *Proc. 30th AIAA Intern.Commun. Satellite Syst. Conference (ICSSC)*, Ottawa, Canada, Sep. 2012. [Online]. Available: http://publications.uni.lu/record/10106/files/

[17] R. Piazza, B. Shankar, and B. Ottersten, "Data predistortion for multicarrier satellite channels using orthogonal memory polynomials," in *Signal Processing Advances for Wireless Communications (SPAWC), 2013 IEEE International Workshop on*, June 2013. [Online]. Available: http://orbilu.uni.lu/handle/10993/4861

[18] M. Abi Hussein, V. A. Bohara, and O. Venard, "On the system level convergence of ila and dla for digital predistortion," in *Wireless Communication Systems (ISWCS), 2012 International Symposium on*, Aug 2012, pp. 870 –874.

[19] A. Saleh, "Frequency-independent and frequency-dependent nonlinear models of twt amplifiers," *IEEE Trans. Commun.*, vol. COM-29, no. 11, pp. 1715–1720, Nov. 1981.

[20] V. J. Mathews, *Polynomial Signal Processing*. New York: Wiley, 2000.

[21] M. H. Hayes, *Statistical Digital Signal Processing and Modeling*. New York:Wiley, 1998.

Roberto Piazza (S'13) received Masters in Electrical Engineering and Computer Science from both the Polytechnic of Turin and the University of Illinois at Chicago in 2010. He was a functional test engineer in Thales Alenia Space from 2010 to 2011. Since 2012 he is pursuing his PhD at the University of Luxembourg in satellite communication. His research interests include signal processing for satellite communication with focus on polynomial signal processing, adaptive filters, channel estimation, channel predistortion and equalization.

Bhavani Shankar M. R. (M'11) received Masters and Ph. D in Electrical Communication Engineering from Indian Institute of Science, Bangalore in 2000 and 2007 respectively. He was a Post Doc at the ACCESS Linnaeus Centre, Signal Processing Lab, Royal Institute of Technology (KTH), Sweden from 2007 to September 2009 and is currently a Research Scientist at SnT. He was with Beceem Communications, Bangalore from 2006 to 2007 as a Staff Design Engineer working on Physical Layer algorithms for WiMAX compliant chipsets. He was a visiting student at the Communication Theory Group, ETH Zurich, headed by Prof. Helmut Blcskei during 2004. Prior to joining Ph. D, he worked on Audio Coding algorithms in Sasken Communications, Bangalore as a Design Engineer from 2000 to 2001. He is currently on the executive committee of the IEEE Benelux joint chapter on communications and vehicular technology. His research interests include statistical signal processing, wireless communications, resource allocation, game theory and fast algorithms for structured matrices.

Björn Ottesten (S'87-M'89-SM'99-F'04) was born in Stockholm, Sweden, in 1961. He received the M.S. degree in electrical engineering and applied physics from Linköping University, Linköping, Sweden, in 1986 and the Ph.D. degree in electrical engineering from Stanford University, Stanford, CA, in 1989.

Dr. Ottersten has held research positions at the Department of Electrical Engineering, Linköping University, the Information Systems Laboratory, Stanford University, the Katholieke Universiteit Leuven, Leuven, and the University of Luxembourg. During 96/97, he was Director of Research at ArrayComm Inc, a start-up in San Jose, California based on Ottersten' s patented technology. He has co-authored journal papers that received the IEEE Signal Processing Society Best Paper Award in 1993, 2001, 2006, and 2013 and 3 IEEE conference papers receiving Best Paper Awards. In 1991, he was appointed Professor of Signal Processing at the Royal Institute of Technology (KTH), Stockholm. From 1992 to 2004, he was head of the department for Signals, Sensors, and Systems at KTH and from 2004 to 2008, he was dean of the School of Electrical Engineering at KTH. Currently, he is Director for the Interdisciplinary Centre for Security, Reliability and Trust at the University of Luxembourg. As Digital Champion of Luxembourg, he acts as an adviser to European Commissioner Neelie Kroes.

Dr. Ottersten has served as Associate Editor for the IEEE TRANSACTIONS ON SIGNAL PROCESSING and on the editorial board of *IEEE Signal Processing Magazine*. He is currently editor in chief of *EURASIP Signal Processing Journal* and a member of the editorial boards of *EURASIP Journal of Applied Signal Processing* and *Foundations and Trends in Signal Processing*. He is a Fellow of the IEEE and EURASIP and a member of the IEEE Signal Processing Society Board of Governors. In 2011, he received the IEEE Signal Processing Society Technical Achievement Award. He is a first recipient of the European Research Council advanced research grant. His research interests include security and trust, reliable wireless communications, and statistical signal processing.